Bulletin of the Seismological Society of America, Vol. 74, No. 4, pp. 1361–1380, August 1984

FORESHOCKS (1966–1980) IN THE SAN ANDREAS SYSTEM, CALIFORNIA

BY LUCILE M. JONES*

ABSTRACT

The spatial and temporal distributions of seismicity preceding moderate ($M_L \geqq 5.0$) main shocks in the San Andreas fault system in California have been analyzed to recognize and characterize the patterns of foreshock occurrence. Of 20 main shocks in the San Andreas system, 7, or 35 per cent, have been preceded by immediate foreshock sequences that included events within 1 day and 5 km of the main shocks. A possible correlation of the rate of foreshock occurrence with type of faulting was found such that none of the four main shocks with reverse faulting had foreshocks while 44 per cent of the strike-slip earthquakes had foreshocks. Some enhanced seismic activity was also observed at relatively large distances from the main shock (13 to 30 km) 1 to 5 days before 40 per cent of the main shocks but this activity cannot be clearly distinguished from the background seismicity. Of the seven immediate foreshock sequences, only two had the swarm-like appearance of the class II foreshocks defined by Mogi. The other foreshock sequences appear to be single events (sometimes with their own aftershocks) preceding the respective main shocks. Four of these sequences are spatially correlated with distinct physical discontinuities in their faults between the hypocenters of the foreshock and main shock, and similar discontinuities may also be associated with the other sequences. The durations of the foreshock sequences were found to decrease as the depths of the main shocks increase from 3 to 11 km, which has been interpreted as a dependence on stress. To account for this stress dependence of the duration and the presence of discontinuities, a model for foreshocks occurrence is presented. This model proposes that foreshocks may represent a process of delayed multiple rupture and that the delay between occurrence of foreshock and main shock might represent the time needed for static fatigue to break the stronger rock at the discontinuity in the fault.

INTRODUCTION

What foreshocks are and why they occur before some but not all main shocks has long been an unresolved question in seismology (e.g., Richter, 1958). Mogi (1963) classified the types of seismicity observed in Japan and included foreshocks in his class II seismicity. This showed Japanese foreshocks as swarm-like events with several earthquakes of similar magnitude preceding the main shock. This has become the standard model of foreshocks so that when a swarm is observed the chances of it being a foreshock sequence are often evaluated (e.g., Aki, 1981; Xu *et al.*, 1982; Yamashina, 1981). However, Utsu (1970) showed that many Japanese foreshocks are single events, sometimes with their own aftershocks that he called class Ib foreshocks, rather than swarms. In California, while some foreshock sequences (like that before the 1972 Bear Valley event) are swarm-like, many other foreshock sequences (like those before the 1968 Borrego Mountain and the 1970 Lytle Creek earthquakes) appear to be single events or class Ib foreshocks so that swarm-like activity may not be the only type of foreshock activity in California.

Although many individual foreshock sequences in California have been recognized

* Present address: U.S. Geological Survey, Seismological Laboratory, California Institute of Technology, Pasadena, California 91125.

and studied (e.g., Ellsworth, 1975; Lindh *et al.*, 1978; Bakun and McEvilly, 1979), the patterns of foreshock occurrence in California have not yet been classified. Moreover, it is not yet established how often foreshocks occur in California. Kagan and Knopoff (1978), using statistical methods, found that California may have anomalously few foreshock sequences but reported that their data set was too small for the results to be statistically valid. Therefore, one goal of this study is to analyze using deterministic methods, the distribution of seismicity prior to main shocks in the San Andreas system in California to classify the type of foreshocks and to determine how often they occur.

Most of the theories for foreshock occurrence assume that heterogeniety of the crust contributes to foreshock occurrence. This was first proposed by Mogi (1963) based in part on laboratory experiments which showed that a homogeneous rock would fracture relatively uniformly but a more heterogeneous rock would exhibit more microcracking before the fracture. Several models have been proposed since then to explain in more detail how the heterogeneity leads to foreshocks. One common explanation (e.g., Jones and Molnar, 1979; Kanamori, 1981) has been that the heterogeneity of the fault plane results in accelerating premonitory slip such as has been documented in the laboratory (Dieterich, 1979). Das and Scholz (1982) suggested that foreshocks may result from localized decrease in rock strength within the initiation zone of the main shock. They also suggested, as did Fukao and Furumoto (1975), that foreshocks could represent a process of delayed multiple rupture. High-quality recordings that are now available for earthquakes in California and recent work on the state of stress in the San Andreas have provided a basis for studying the details of foreshock sequences. The data from California are examined in this paper to determine which, if any, model is most compatible with the observed foreshocks.

Data

The main shock data set used in this study is the set of all earthquakes with $M_L \geqq 5.0$ that occurred in the San Andreas physiographic province (as defined by Zoback and Zoback, 1980) from 1966 to 1980. (This is all of California, except for the Sierra Nevada. This region has been excluded because the data from there are not of as high quality as the San Andreas data and because the extensional tectonics of the region might produce different types of foreshock sequences.) The 20 events in this category are plotted in Figure 1 and their hypocentral parameters listed in Table 1. Since several seismic networks record earthquakes in California, three catalogs of earthquakes have been used to search for possible changes in seismicity before these main shocks. For earthquakes in southern California (south of 36°N latitude), the catalog of the CIT/USGS network in southern California was used. The seismicity before main shocks in northern California (north of 36°N latitude) after 1971 was studied using the records of the CALNET seismic network operated by the USGS. Since CALNET was not fully operational before 1971, seismicity in northern California before that time was taken from the California Division of Mines and Geology Earthquake Catalogue of California (Real *et al.*, 1978) which includes earthquakes reported both by CALNET and the seismic network of the University of California, Berkeley. By using these three catalogs, the record before each of the main shocks should be as complete as possible. Table 1 shows which catalog was used for each earthquake. All magnitudes in this paper are M_L from these catalogs.

To search for patterns of foreshock occurrence, the seismicity before each main

shock is examined over a larger time and space window than that expected to be occupied by the possible precursory seismicity so that a change in activity can be compared to some background level. This study is concerned with immediate foreshocks such as those discussed by Mogi that occur within hours, days, or at most weeks of the main shock. The occurrence of longer term changes in activity,

FIG. 1. Map of the San Andreas fault system, California, showing major faults (from geologic map of California, 1972) and the location of the main shocks listed in Table 1. Main shocks with foreshocks are shown by closed circles, and main shocks without foreshocks are shown by open circles.

something that occurs over years, is not considered here. A year of seismicity before each of the main shocks was examined, including all events within a 30 km radius (approximately the maximum length of rupture for main shocks of the size considered here) of the epicenter of the main shock. For uniformity in reporting before all of the main shocks, only events of $M_L \geqq 2.0$ are included. This may be slightly lower than the threshold of completeness for some of the earlier main shocks, but any higher threshold would too greatly limit the magnitude differential available between main shocks and possible foreshocks.

TABLE 1

MODERATE ($M_L \geqq 5.0$) MAIN SHOCKS IN THE SAN ANDREAS (1966–1980)

Main Shock	Location	Magnitude	Depth	Catalog*	Source
Parkfield 28 June 1966	35° 57.50′ 120° 30.00′	5.5	7.5	1	Lindh and Boore, 1981 Aki, 1979
Watsonville 28 Sept. 1967	37° 0.60′ 121° 47.30′	5.3	8.0	1	
Borrego Mountain 9 Apr. 1968	33° 9.20′ 116° 6.23′	6.4	11.1	3	Allen and Nordquist, 1972 Corbett and McNalley, 1981
Coyote Creek 28 Apr. 1969	33° 20.60′ 116° 20.78′	5.8	20.0	3	
Santa Rosa 2 Oct. 1969	38° 28.20′ 122° 41.40′	5.6	11.0	1	
Lytle Creek 12 Sept. 1970	34° 15.79′ 117° 34.36′	5.4	8.8	3	This study
San Fernando 9 Feb. 1971	34° 24.67′ 118° 24.04′	6.4	8.4	3	
Superstition 30 Sept. 1971	33° 2.01′ 115° 49.24′	5.1	8.0	3	
Bear Valley 24 Feb. 1972	36° 34.13′ 121° 11.29′	5.0	6.5	2	Ellsworth, 1975
Point Magu 21 Feb. 1973	34° 3.89′ 119° 2.10′	5.9	8.0	3	
Thanksgiving 28 Nov. 1974	36° 54.13′ 121° 36.39′	5.0	7.0	2	
Galway Lake 1 June 1975	34° 30.70′ 116° 29.72′	5.2	2.8	3	This study
Santa Barbara 13 Aug. 1978	34° 20.82′ 119° 41.76′	5.1	13.0	3	
New Year's 1 Jan. 1979	33° 56.66′ 118° 40.88′	5.0	11.3	3	
Homestead 15 Mar. 1979	34° 19.68′ 116° 26.63′	5.2	5.0		Hutton *et al.*, 1980 Stein and Liwoski, 1983
Coyote Lake 15 Oct. 1979	37° 6.59′ 121° 30.68′	5.9	7.0	2	
Imperial Valley 15 Oct. 1979	32° 36.82′ 115° 19.09′	6.6	12.3	3	
Livermore 24 Jan. 1980	37° 49.63′ 121° 48.13′	5.8	10.2	2	Scheimer and Cocheram, 1982, Bolt *et al.*, 1981
Anza 25 Feb. 1980	33° 30.06′ 116° 30.79′	5.5	13.6	3	
Eureka 8 Nov. 1980	41° 7.03′ 124° 39.89′	7.0	10.0	2	

* 1, California Division of Mines and Geology; 2, CALNET; 3, CIT/USGS.

ANALYSIS

Recognition of Foreshocks

The seismicity preceding each of the main shocks is shown in Figure 2. The time before the main shock when the event occurred is plotted against its distance from the main shock for each main shock separately. On the basis of these distributions of seismicity, the main shocks are divided into three categories, those with foreshocks immediately before the main shock near the epicenter of the main shock (Figure 2a), those with some enhanced seismic activity at relatively large distances from the main shock (Figure 2b), and those without any identifiable change in seismicity (Figure 2c).

To compare the rate of foreshock occurrence with the rate of background seismicity, the activity within 30 km radii circles centered at the epicenters of each of the 20 main shocks for the period of time 100 to 300 days before each main shock is assumed to represent the background rate of seismicity. The average rate of occurrence ($M_L \geqq 2.0$) in these circles is 4.1×10^{-5} events/day/km^2. The rate of activity in different regions ranges from 1.8×10^{-6} events/day/km^2 around the Santa Rosa and Eureka main shocks to 1.2×10^{-4} events/day/km^2 around the Imperial Valley and Galway Lake main shocks.

The seven main shocks with immediate foreshocks (Figure 2a) all have earthquakes within 1 day and 5 km of the occurrence of the main shock. Based on the calculated background rate, the chance of an event occurring randomly within a 5 km radius circle on a given day is 0.32 per cent. For 20 main shocks, there is thus a 6 per cent chance that one event would occur randomly within 1 day and 5 km of one of the main shocks. The 30 events recorded within 1 day and 5 km of 7 main shocks represent a rate of occurrence that is 500 times larger than the background rate.

None of the other 13 main shocks (Figure 2, b and c) are associated with such a sudden jump in activity prior to their occurrence. Although the seven main shocks in Figure 2b are preceded by some enhanced seismicity, these earthquakes are not clearly anomalous like the immediate foreshocks discussed above because a larger time and space window is involved. All of these main shocks were preceded by 1 to 5 days by another event located 13 to 30 km away from the main shock. The random chance of having an earthquake in 5 days in a circle with a radius of 30 km (from the above background rate) is 58 per cent. Thus in 20 such circles, one would expect 12 events from background occurrence; in fact, aside from the immediate foreshocks, 12 events were recorded in these 20 circles. Moreover, most theories of foreshocks (e.g., Jones and Molnar, 1979; Das and Scholz, 1981) assume that foreshocks occur on the same fault that slips during the main shock (which is reported for the seven immediate foreshock sequences, as will be discussed below). Most of the distant events in Figure 2b did not occur on the same section of the fault that slipped during the main shock including those preceding the Watsonville, Coyote Creek, Imperial Valley, Coyote Lake, and Santa Barbara earthquakes. Because of the different faults involved and the higher background level of activity in the 30 km radii, it is less likely that these distant events are related to the main shocks. No change in seismicity can be seen before the six main shocks in Figure 2c.

Thus, 7 of 20, or 35 per cent, of the main shocks of $M \geqq 5.0$ in the San Andreas physiographic province have been preceded by immediate foreshock sequences. Of course, this result is dependent upon the detection level of the local seismic network. Although the detection capabilities in California have increased significantly since 1966, the rate of foreshock occurrence has not (note that the 1966 to 1970 rate is

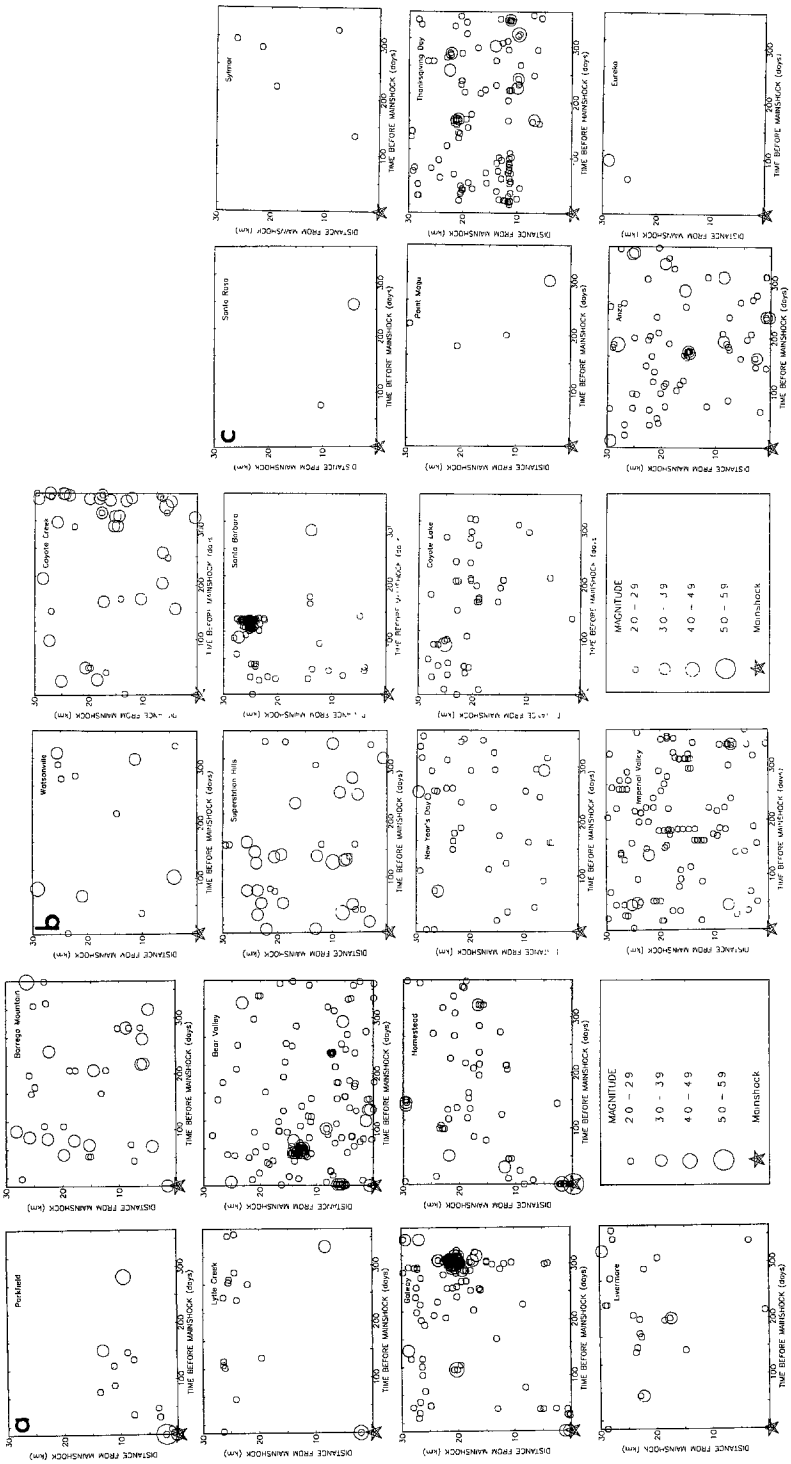

FIG. 2. All of the earthquakes listed in the catalogs (see text) within 30 km of the epicenter of the main shock and that occurred within 1 yr of the main shock. For each main shock individually, the time before the main shock is plotted against the distance from the main shock. (a) Shows main shocks with foreshocks; (b) shows main shocks with some long-distance precursory seismic activity; and (c) shows main shocks without short-term seismic precursors.

50 per cent); hence, this is not considered a significant problem. It should also be noted that there is a regional variation in the rate of foreshock occurrence. None of the earthquakes on the reverse faults in the Transverse Ranges (Sylmar, Point Magu, Santa Barbara, and New Year's Day) have been preceded by foreshocks, while 44 per cent of the main shocks on strike-slip faults of the San Andreas have had foreshocks. The enhanced seismicity shown in Figure 2b is seen before both reverse and strike-slip events.

Characteristics of Foreshocks

The seven sequences of immediate foreshocks (Figure 2a) all include an event within 5 km and 1 day of the main shock which could be used as a criteria for

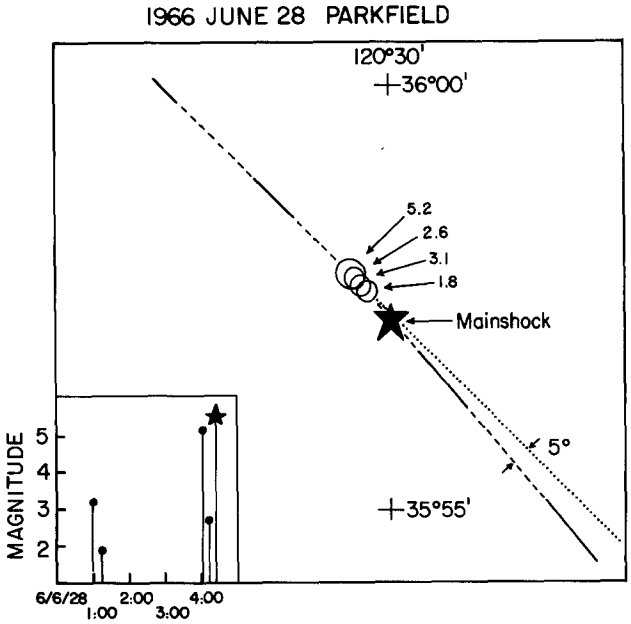

FIG. 3. The spatial distribution of the foreshocks (circles) and main shock (star) of the Parkfield foreshock-main shock sequence. The details of the San Andreas fault are also shown. The dotted line shows the projection of the strike of the northern section of the fault onto the section south of the bend. The difference in strike is 5° (from Lindh and Boore, 1981). The *inset* shows a plot of time versus magnitude for the foreshocks and main shock.

defining foreshocks in the San Andreas system. The temporal and spatial distribution of each of these foreshock sequences is described below. In some cases, relative relocations of the foreshock-main shock sequences have been carried out [see Jones *et al.* (1982) for a discussion of this technique].

Parkfield, 28 June 1966. This earthquake occurred on the central section of the San Andreas fault just at the southern end of the creeping section. Lindh and Boore (1981) have noted that there is a change in strike of the San Andreas fault of about 5° just north of the epicenter of the main shock (Figure 3). A cluster of immediate foreshocks was located just north of this change in strike starting 3.5 hr before the main shock. The largest of these foreshocks was a $M_L = 5.1$ event that occurred 17 min before the main shock; the rest of the events were $M \leqq 3.1$. Three events of $M \simeq 2$ recorded in May and early June north of these foreshocks and are not considered

part of the foreshock sequence since they occurred in the seismically active creeping section of the San Andreas fault.

Borrego Mountain, 9 April 1968. The Borrego Mountain earthquake was located on the San Jacinto fault just north of a large en-echelon step in the fault, the Octillo Badlands (Allen and Nordquist, 1972). The hypocenter is east of the surface fault strand that was offset in the event (Figure 4). Surface rupture and aftershocks were observed both north and south of the Octillo Badlands so it appears that rupture propagated through the offset. One foreshock of $M = 3.7$ occurred 80 sec before the

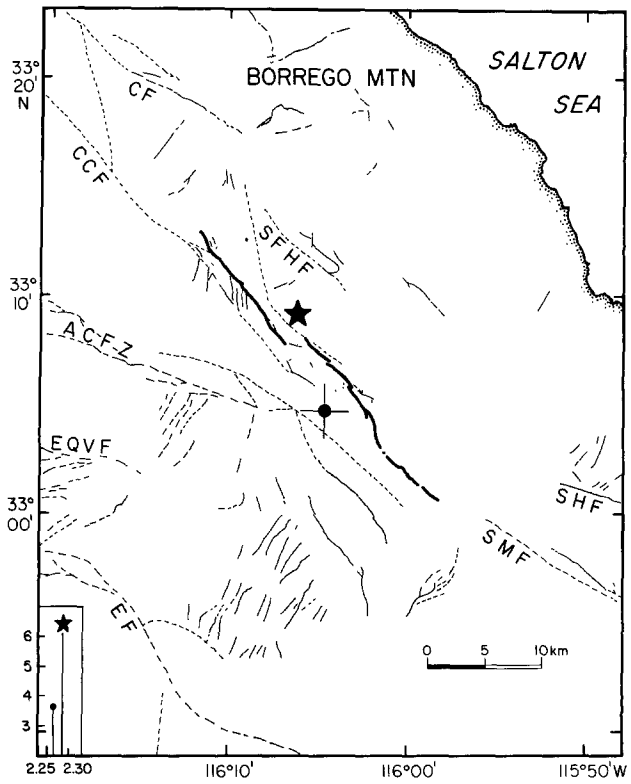

FIG. 4. The spatial distribution of the foreshock (circle) and main shock (star) of the Borrego Mountain foreshock-main shock sequence. The details of the San Jacinto fault are also shown (from Wyss and Hanks, 1972). The location of the main shock is from Corbett (1981); the foreshock was relocated relative to the master (this study). The *inset* shows a plot of time versus magnitude for the foreshock and main shock.

main shock. Relative relocation of the event with respect to the main shock (this study) shows that the foreshock occurred significantly to the south of the main shock across the en-echelon step.

Lytle Creek, 12 September 1970. The epicenter of the Lytle Creek main shock is not clearly associated with any fault, but lies between the San Andreas and the San Jacinto faults near the intersection of these two faults. No detailed study of this earthquake has been published, but relative relocation of the main shock with respect to the Lytle Creek earthquake of 19 October 1979 has provided a reasonably accurate hypocentral location (this study; Table 1). Locations of the aftershocks by Hanks (unpublished data) do not define a simple planar feature, although they are compatible with occurrence on a fault parallel to the San Andreas and San Jacinto

faults (Figure 5). The main shock was preceded by two foreshocks 20 min before it, a $M = 4.2$ event with its own aftershock of $M = 2.4$ (Figure 5). The largest foreshock is 2 km away from the main shock, perpendicular to the trend of the aftershocks. However, it is not clear if this is a real feature of the rupture zone.

Bear Valley, 24 February 1972. Ellsworth (1975) showed that the main shock occurred on the central creeping section of the San Andreas fault and that the aftershocks which preceded the main shock for 2 days were located on a separate, small fault conjugate to the San Andreas. Although this area of the fault is seismically very active, there is a clear start to the foreshock sequence by a $M = 3.4$

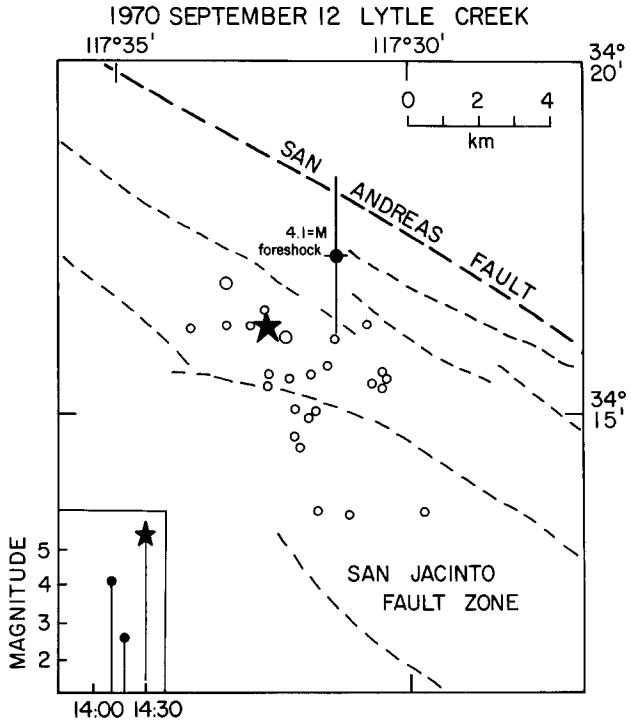

FIG. 5. The locations of the main shock (star), aftershocks (open circle), and largest foreshock (closed circle) of the Lytle Creek sequence. The San Andreas fault and strands of the San Jacinto fault zone are shown. The locations of the main shock and aftershocks are from Hanks (unpublished study) and that of the foreshock is a location relative to the main shock (this study). The *inset* shows a plot of time versus magnitude for the foreshocks and main shock.

event (Figure 6). Only two $M \simeq 3$ foreshocks occurred almost at the epicenter of the main shock in the minute before it occurred.

Galway Lake, 1 June 1975. The Galway Lake earthquake caused surface rupture on a small north-south trending fault in the Mojave desert which was mapped by Hill and Deeby (1977) who found a change in strike of the fault of a few degrees (Figure 7). The hypocenter of the main shock was exceptionally shallow (2.8 km) as were those of all of its foreshocks and aftershocks. The main shock was preceded by several weeks of foreshock activity all within a few kilometers of the main shock. The first $M \geqq 2.0$ foreshock was recorded 40 days before the main shock, but a $M = 1.9$ event also occurred almost 12 weeks before the main shock on 9 March 1975 in the same region which might be the start of the foreshock sequence (Figure 7). The two largest foreshocks preceded the main shock by less than 1 hr. Absolute

locations of them and the main shock place them north and south, respectively, of the change in strike of the fault mentioned above. In addition, Lindh *et al.* (1978), showed that there was a change in the fault plane solution between the foreshocks and main shock consistent with this change in strike of the fault.

Homestead, 15 March 1979. This earthquake sequence appears to have activated two almost perpendicular faults (north-south and east-west trending) in the Mojave desert (Hutton *et al.*, 1980). The whole sequence is sometimes considered a swarm because there were four earthquakes of $M \simeq 5$ in the sequence, but in this study,

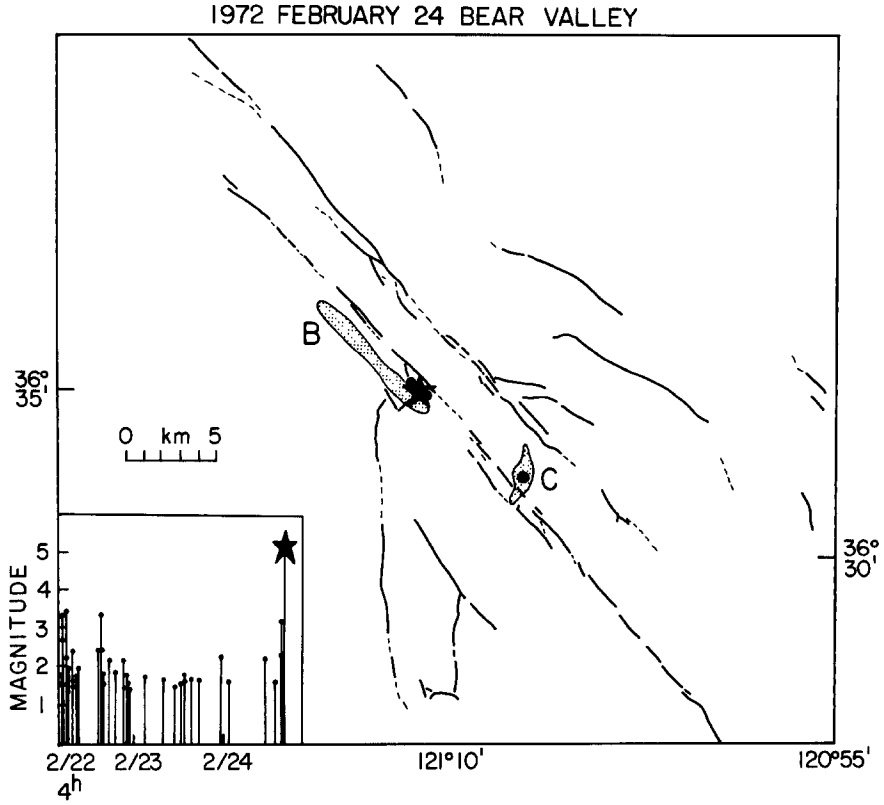

FIG. 6. The spatial distribution of the foreshocks and main shock of the Bear Valley foreshock-main shock sequence. The first foreshock and the last two foreshocks are shown by circles and the main shock by a star. The rest of the foreshocks were located within region A. Region B is the area of the aftershocks. The details of the San Andreas fault are also shown (from Ellsworth, 1975). The *inset* shows a plot of time versus magnitude for the foreshocks and main shock.

the largest earthquake is taken as the main shock. It was preceded by 20 min by a large foreshock ($M = 4.9$) which had its own aftershock sequence. The foreshocks and main shock occurred on the same fault but the second fault intersected the main fault between the hypocenters of the largest foreshock and main shock (Figure 8). Fault plane solutions of the largest foreshock and main shock (Hutton *et al.*, 1980) also show a change in strike of the main fault plane of 7° between the two events.

Livermore, 24 January 1980. This earthquake sequence occurred on a small fault subparallel to the San Andreas in the Livermore Valley. One foreshock preceded the main shock by 90 sec occurring almost directly above the main shock within a few hundred meters (Scheimer and Cocheram, 1981). There were two groups of

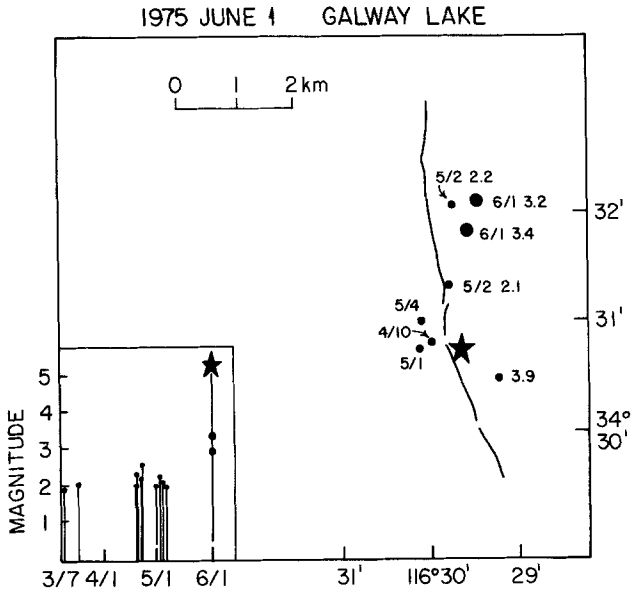

FIG. 7. The locations of the main shock (star), and foreshocks (closed circles) of the Galway Lake sequence. The Galway Lake fault as mapped from surface rupture during this sequence by Hill and Deeby (1977) is also shown. The locations of the main shock and foreshocks are absolute locations (this study). The *inset* shows a plot of time versus magnitude for the foreshocks and main shock.

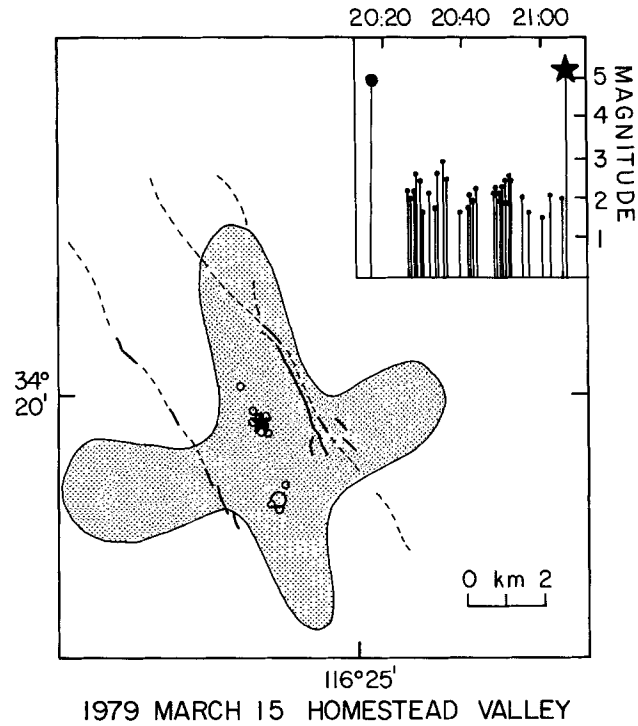

FIG. 8. The spatial distribution of the Homestead Valley sequence. The stippled region is the area of aftershocks, the circles are foreshocks, and the star is the main shock. The heavy line is the surface rupture during the sequence (from Hutton *et al.*, 1979). The *inset* shows a plot of time versus magnitude for the foreshocks and main shock.

aftershocks, one located directly above the hypocenter of the main shock and one extending south from the main shock along the fault, confined to approximately the same depth as the main shock, 9 to 12 km (Figure 9). Thus, there is a suggestion that both the main shock and the foreshock could have occurred at the intersection of two faults.

Summary. Five of the seven foreshock sequences begin in the last day before the main shock. All of these sequences have either only one foreshock (Borrego Mountain and Livermore) or one large foreshock with its own aftershocks (Parkfield, Lytle Creek, and Homestead). (The Homestead sequence overall appeared more like a swarm, but the events before the main shock were one large event with aftershocks.) The Bear Valley foreshock sequence preceded the main shock by 58 hr and appeared more swarm-like with 14 events of $2.0 \leqq M \leqq 3.5$ in the sequence. The Galway Lake foreshock sequence also had a swarm-like character with a gradual increase in number and magnitude of the events. Thus, of seven sequences,

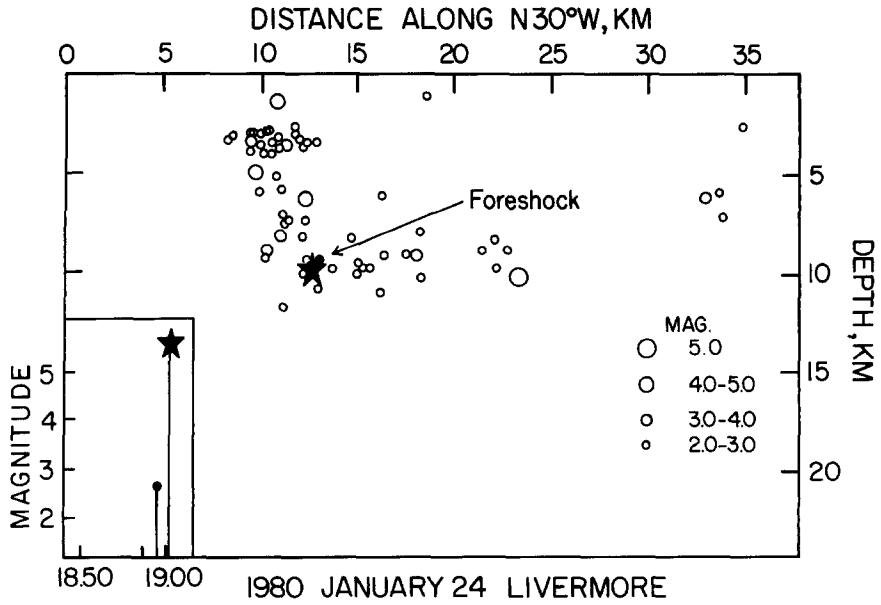

FIG. 9. The depth distribution of the Livermore Valley sequence. The projections of the main shock (star), aftershocks (open circle), and foreshock (closed circle) along the stroke of the aftershock zone are shown (from Scheimer and Cocheram, 1981). The *inset* shows a plot of time versus magnitude for the foreshocks and main shock.

only two, or 10 per cent of all the main shocks, had foreshocks similar to those described by Mogi. One sequence, Homestead, could be a class IIIa sequence [as modified by Utsu (1970)] or multiple main shocks. The remaining four foreshock sequences are single events, sometimes with their own aftershocks, or the class Ib foreshocks of Utsu (1970).

Four of the foreshock sequences had discontinuities in the fault surface between the foreshocks and main shocks. Parkfield had a change in strike, Borrego Mountain had an en-echelon step, and Bear Valley and Homestead had intersecting faults. The other three sequences also had possible discontinuities in their faults. This suggests that the physical discontinuities in the faults may be related to the occurrence of the foreshocks and is in agreement with previous findings that the

geometry of fault zones can play an important role in determining seismicity patterns (Bakun *et al.*, 1980; Bakun, 1980).

Magnitudes

The magnitudes of the largest foreshocks are plotted against the magnitudes of the main shocks in Figure 10a. As was found in a worldwide study of foreshocks (Jones and Molnar, 1979), the magnitudes of the foreshocks do not seem to be related to those of the main shocks. In addition, the magnitudes of the foreshocks do not seem to be related to the time between the foreshocks and main shocks (Figure 10b).

Main Shock Depth and Duration of Sequence

The durations of the foreshock sequences vary from 80 sec at Borrego Mountain to perhaps as much as 12 weeks at Galway Lake. Although the duration of a sequence does not depend on the magnitude of the foreshock (Figure 10), there does seem to be a relationship between the depth of the main shock and the time between the earliest foreshock and the main shock. In Figure 11, the depth of the main shock is plotted against the logarithm of the duration of the foreshock sequence. With the exception of the Homestead sequence, the logarithm of the duration of the foreshock sequence decreases linearly as the depth of the main shock increases.

Of the parameters that vary with depth, the stress state is one of the most likely to affect the occurrence of earthquakes. McGarr *et al.* (1982) have estimated the variation in minimum compressive stress with depth near the San Andreas from measurements in the top kilometer of the crust as

$$\sigma_1 = 2.90 \pm 0.60 + (19.28 \pm 1.52)^* z \tag{1}$$

where σ_1 is in MPa and z is in kilometers. The stress calculated from this relationship is shown with the depths in Figure 11. Hence, the durations of the foreshock sequences are inferred to decrease with increasing stress.

INTERPRETATION

To understand how the depth of the main shock could be affecting the duration of the foreshock sequences, the relationships between the stresses close to failure in the fault zone need to be examined. Failure in brittle materials, either fracture of the material or frictional sliding on a preexisting surface, obeys Coulomb's Law (e.g., Jaeger and Cook, page 95, 1976);

$$\sigma_s = C + q \cdot \sigma_1 \tag{2}$$

where σ_3 and σ_1 are the maximum and minimum principal effective stresses, respectively, C is the cohesion, and q is the coefficient of friction. In addition, failure can occur at lower stresses than those given above for instantaneous failure, by the process of static fatigue (e.g., Scholz, 1972). The rock will not fail instantaneously after the application of these lower stresses but will after a period of time that depends on the ratio of the applied stress to the instantaneous strength, or

$$t = T \exp\left(\frac{-\kappa\sigma}{\sigma_c}\right) \tag{3}$$

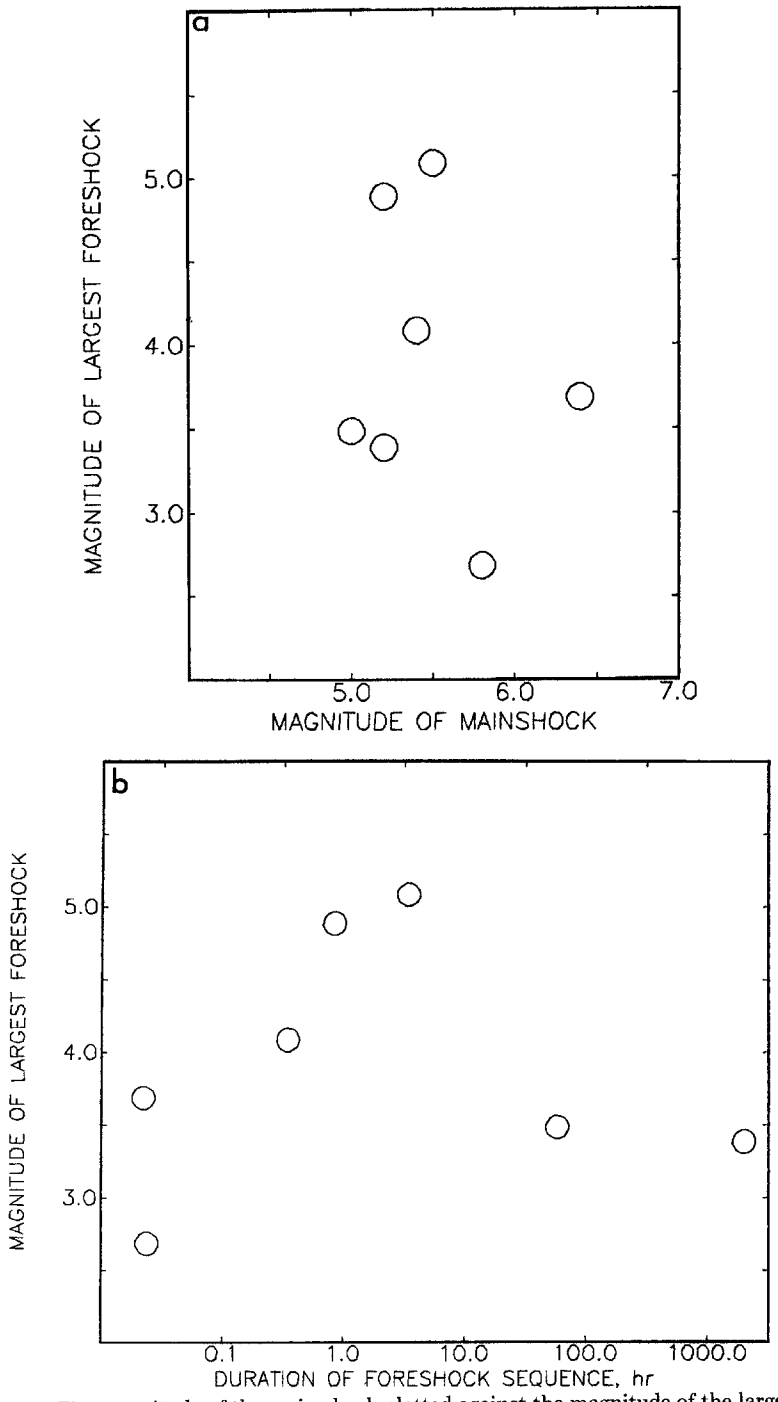

FIG. 10. (a) The magnitude of the main shock plotted against the magnitude of the largest foreshock for the seven foreshock-main shock sequences in the San Andreas. (b) The magnitude of the largest foreshock plotted against the logarithm of the duration of the foreshock sequence for the seven sequences in the San Andreas.

where T and κ are constants, t is the time to failure, σ is the applied maximum principal stress, and σ_c is the maximum principal stress needed for instantaneous failure [which is a function of pressure by equation (2). There is also a slight additional effect of confining pressure which increases the time needed as pressure

increases but this effect is not very strong when the rock is saturated with water (Kranz, 1980).] The equation above is valid for fracture of brittle materials but a similar failure mode has been recognized in frictional deformation (Dieterich, 1981).

The proposed model for foreshock occurrence assumes that the strength of the future rupture surface of the main shock is variable [i.e., that C and q in equation (2) are functions of position along the fault] such that the discontinuities in the faults (seen for the foreshock-main shock sequences, Figures 3 to 10) would be the strongest parts of the faults and the foci of the main shocks. The strength of the

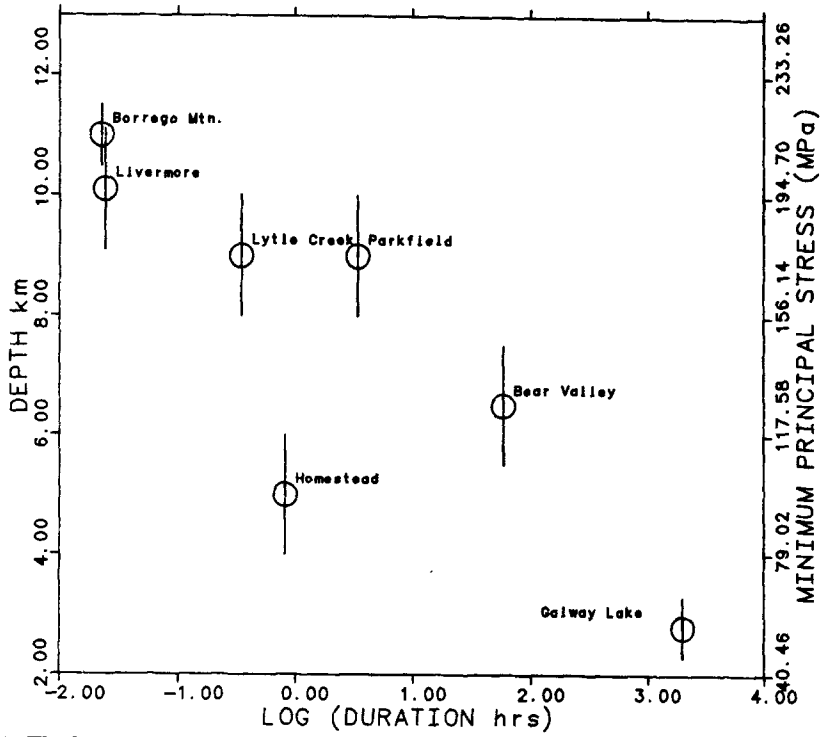

FIG. 11. The logarithm of the duration of the foreshock sequences in hours versus the depth of the main shock. Also shown is the minimum principal stress calculated for those depths from the relation of McGarr *et al.* (1982). For the Galway Lake sequence, the duration shown is from the first $M = 1.9$ foreshock.

fault at the main shock foci would be given by

$$\sigma_{Sm} = C_m + q_m \cdot \sigma_1. \tag{4}$$

Suppose a nearby section is somewhat weaker with a strength of

$$\sigma_{Sf} = C_f + q_f \cdot \sigma_1 \tag{5}$$

where $C_f < C_m$ and $q_f \leqq q_m$. As the shear stress on the fault increases, the failure strength of the weaker patch will be reached first. If the failure of this weaker section is unstable, an earthquake (foreshock) will occur, loading the nearby discontinuity with a stress at the failure strength of the weaker section [given by equation (5)]. If the differences in strength between the two regions is sufficiently large, failure will not occur instantaneously but the process of static fatigue will be accelerated. The time to failure (duration of the foreshock sequence) by equation (3) will depend on the ratio of failure strengths of the source regions of the foreshock and main shock foci.

Combining equations (1), (4), and (5), the ratio of strengths is

$$\frac{\sigma_{Sf}}{\sigma_{Sm}} = \frac{S_f + q_f \cdot (2.9 + 19.29 \cdot z)}{S_m + q_m \cdot (2.9 + 19.28 \cdot z)}. \tag{6}$$

Thus the ratio (and hence the duration of the foreshock sequence) depends on the cohesions and coefficients of friction of both the stronger and weaker patches and the depth. The depth dependence is quite strong because of the large increase in minimum compressive stress with depth.

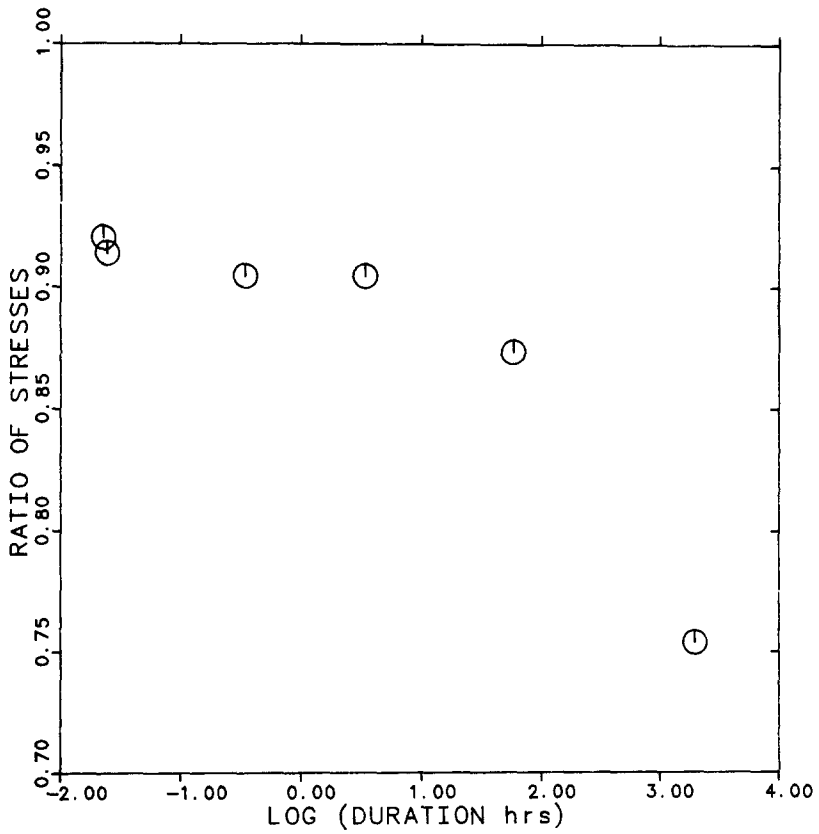

FIG. 12. The ratio of maximum principal effective stresses needed for failure of a weak patch of the fault divided by that needed for failure of a strong patch versus duration of the foreshock sequence.

To examine the depth dependence, a test case has been calculated where the weaker patch (the foreshock focus) has a strength of $\sigma_3 = 0 + 4.04 \cdot \sigma_1$ (Byerlee's Law) while the stronger patch has some cohesion for a strength of $\sigma_3 = 85$ MPa + $4.04 \cdot \sigma_1$. This ratio of strengths has been calculated for the depths of each of the seven foreshock-main shock sequences (Table 1) and plotted against the logarithm of the durations of the foreshock sequences in Figure 12. This relationship between ratio and duration is in general agreement with laboratory results. For instance, for dry Barre granite, Kranz (1980) found that the time to failure would be 1 min to 1 hr for applied stresses that were 90 per cent of the instantaneous fracture strength and on the order of months for 70 per cent of the instantaneous fracture strength.

Thus, static fatigue of rock with variable strength similar to that found in the laboratory could produce the durations of foreshock sequences seen in California.

Discussion

This model could explain why none of the thrust faults in the Transverse Ranges have experienced foreshocks. The stress versus depth relation of McGarr *et al.* (1982) is valid only for the strike-slip faults of the San Andreas system, where the vertical stress is the intermediate principal stress. For thrust faulting, the vertical stress is the least principal stress leading to principal stresses much higher than in a strike-slip regime. Thus, the thrust faults could be discontinuous [such as the proposed down-dip bend in the fault the 1971 Sylmar earthquake, e.g., Heaton (1982)] but the stress on the fault would be too high for the "foreshock" and "main shock" to be separated in time.

This could also explain why the Homestead sequence does not fit in the apparent relationship (Figure 11). The difference in magnitude between foreshock and main shock is much smaller for the Homestead sequence than for the other foreshock sequences. Such a large foreshock could concentrate stress at the hypocenter of the main shock. This stress concentration factor is the total area of the fault that slips in the sequence divided by the area that did not slip in the foreshock (Jones and Molnar, 1979). If the foreshock is small compared to the main shock, this factor is close to 1; for all of the sequences except Homestead it is less than 1.05. Assuming the areas of the earthquakes from the relationship between area and magnitude of Wyss and Brune (1968), the factor for Homestead is 1.6.

Several other models for foreshock occurrence have been proposed but at least two of these models seem to be incompatible with the data presented here. One has suggested that foreshocks could result from accelerating premonitory creep on a frictional surface (e.g., Jones and Molnar, 1979). However, laboratory studies of this process (Dieterich, 1978) have shown that the time from onset of creep to failure increase with increasing stress. While there are large errors in the values of stress assumed here, it is clear that the duration of the sequence does decrease with increasing stress, not increase as in the laboratory experiments, so that just creep does not seem a likely mechanism for producing these foreshocks.

Other models (e.g., Jones *et al.*, 1982) have suggested that increased pore pressure caused by the foreshocks could be triggering the main shock and thus controlling the duration of the foreshock sequences. If this were true, the durations of the sequences should decrease as the magnitudes of the foreshocks increase. No such dependence is seen in these data (Figure 10), suggesting that this model is not applicable to California foreshocks.

While the data presented here are compatible with a foreshock model of delayed multiple rupture, this does not require that all foreshocks everywhere result from the same process. Foreshocks produced by delayed multiple rupture seem more likely when the magnitudes of the foreshocks are relatively large. As noted before, two types of foreshock sequences, swarms and single events, are seen in both the San Andreas and Japan. Das and Scholz (1981) suggested that two processes, delayed multiple rupture and initiation cracking due to localized decreases in strength, could produce foreshocks. If the delayed multiple rupture produces the single foreshocks, perhaps initiation cracking causes swarm-like foreshocks. However, the two Californian sequences with the appearance of swarms, Bear Valley

and Galway Lake, fit the depth-time relation in Figure 11, so more foreshock sequences need to be studied to answer this question.

The generally small temporal spacing between foreshocks and main shocks in the San Andreas system may limit the usefulness of foreshocks in earthquake prediction in that area. However, since the duration of the foreshock sequence is a function of the geometry of the fault and the material properties of the rocks, the duration of the sequence should be the same for different sequences at the same location. Indeed, the temporal distributions of several Parkfield foreshock-main shock sequences have been very similar. Thus, a repeat of the 1857 Fort Tejon earthquake could have the same foreshock distribution as the 1857 event (Sieh, 1978). If these foreshocks could be recognized in time, this might allow a few hours for preparation.

Conclusions

Immediate foreshocks, as a phenomena distinct from background seismicity, have occurred before 35 per cent of the 20 moderate and larger main shocks in the San Andreas system of California. These foreshock sequences can be defined as having an event within 1 day and 5 km of the main shock. None of the four reverse-faulting earthquakes of the Transverse Ranges had foreshocks while 44 per cent of the strike-slip earthquakes did have. Enhanced seismic activity at relatively large distances from the main shock (13 to 30 km) has also preceded 40 per cent of the main shocks by 1 to 5 days but this activity cannot be clearly distinguished from the background seismicity. Of the seven immediate foreshock sequences, only two had the swarm-like appearance of the class II foreshocks defined by Mogi. The other foreshock sequences appear to be single events (sometimes with their own aftershocks) preceding the main shocks. Four of these sequences were correlated with physical discontinuities in their faults between the hypocenters of the foreshock and main shock, and this is also possible for the other four sequences. The durations of the foreshock sequences are found to decrease as the depths of the main shocks increase from 3 to 11 km, which is interpreted as a dependence on stress. This suggests that foreshocks may represent a process of delayed multiple rupture and that the delay between occurrence of foreshock and main shock might represent the time needed for static fatigue to break the stronger rock at the discontinuity in the fault.

Acknowledgments

The author thanks all of those who supplied data from California, including Allan Lindh, Robert Cocheram, Jerry Eaton, Kate Hutton, Carl Johnson, and Art Frankel. This work was supported by NSF Grant EAR82-08387 and by the author's Lamont Postdoctoral Fellowship. Terry Engelder and Egill Hauksson critically reviewed the manuscript.

References

Aki, K. (1979). Characterization of barriers on an earthquake fault, *J. Geophys. Res.* **84,** 6140–6148.

Aki, K. (1981). A probabilistic synthesis of precursory phenomena, in *Earthquake Prediction: An International Review, Maurice Ewing Series, 4,* D. Simpson and P. Richards, Editors, Am. Geophys. Union, Publ., Washington, D.C., 566–574.

Allen, C. R. and J. M. Nordquist (1972). Borrego Mountain earthquake: foreshock, mainshock and larger aftershocks, *U.S. Geol. Surv. Profess. Paper 787,* 16–23.

Bakun, W. H. (1980). Seismic activity on the southern Calaveras fault, *Bull. Seism. Soc. Am.* **70,** 1181–1198.

Bakun, W. H. and T. V. McEvilly (1979). Are foreshocks distinctive? Evidence from the 1966 Parkfield and 1975 Oroville, California sequences, *Bull. Seism. Soc. Am.* **69,** 1027–1038.

Bakun, W. H., R. M. Stewart, C. G. Bufe, and S. M. Marks (1980). Implication of seismicity for a failure of a section of the San Andreas fault, *Bull. Seism. Soc. Am.* **70,** 185–201.

Bolt, B. A., T. V. McEvilly, and R. A. Urhammer (1981). The Livermore, California, sequence of January 1980, *Bull. Seism. Soc. Am.* **71,** 451–463.

Corbett, E. J. and K. C. McNally (1980). Seismicity of the Borrego Mountain region 1960–1968 (abstract), *Earthquake Notes* **50,** 4.

Das, S. and C. H. Scholz (1981). Theory of time-dependent rupture in the earth, *J. Geophys. Res.* **86,** 6039–6051.

Dieterich, J. H. (1978). Time-dependent friction and the mechanics of strike-slip, *Pure Appl. Geophys.* **116,** 790–806.

Dieterich, J. H. (1979). Modeling of rock friction, 1, Experimental results and constitutive equations, *J. Geophys. Res.* **84,** 2161–2168.

Dieterich, J. H. (1981). Constitutive properties of faults with simulated gouge, in *Mechanical Behavior of Crustal Rocks, Geophysical Monograph 24,* Am. Geophys. Union, Publ., Washington, D.C. 103–120.

Ellsworth, W. L. (1975). Bear Valley earthquake sequence of February–March, 1972, *Bull. Seism. Soc. Am.* **65,** 1181–1197.

Fukao, Y. and M. Furumoto (1975). Foreshocks and multiple shocks of large earthquakes, *Phys. Earth Planet. Interiors* **10,** 355–368.

Heaton, T. H. (1982). The 1971 San Fernando earthquake: a double event? *Bull. Seism. Soc. Am.* **72,** 2037–2062.

Hill, R. J. and D. J. Deeby (1977). Surface faulting associated with the 5.2 magnitude Galway Lake earthquake of May 31, 1975: Mojave Desert, San Bernardino County, California, *Geol. Soc. Am. Bull.* **88,** 1378–1384.

Hutton, L. K., C. E. Johnson, J. C. Pechman, J. E. Ebel, J. W. Given, D. M. Cole, and P. T. German (1980). Epicentral locations for the Homestead Valley earthquake sequence, March 15, 1979, *Calif. Geol.* **33,** 110–114.

Jaeger, J. C. and N. G. W. Cook (1976). *Fundamentals of Rock Mechanics,* Halstead Press, New York, 450 pp.

Jones, L. M. and P. Molnar (1979). Some characteristics of foreshocks and their possible relation to earthquake prediction and premonitory slip on faults, *J. Geophys. Res.* **84,** 5709–5723.

Jones, L. M., B. Q. Wang, S. X. Xu, and T. J. Fitch (1982). The foreshock sequence of the February 4, 1975 Haicheng, China earthquake, *J. Geophys. Res.* **87,** 3444–3455.

Kagan, Y. and L. Knopoff (1978). Statistical study of the occurrence of shallow earthquakes, *Geophys. J. Roy. Astr. Soc.* **55,** 67–86.

Kanamori, H. (1981). The nature of seismicity patterns before large earthquakes, in *Earthquake Prediction: An International Review, Maurice Ewing Series, 4,* D. Simpson and P. Richards, Editors, Am. Geophys. Union, Publ., Washington, D.C., 1–19.

Kranz, R. L. (1980). The effects of confining pressure and stress difference on static fatigue of granite, *J. Geophys. Res.* **85,** 1854–1866.

Lindh, A., G. Fuis, and C. Mantis (1978). Foreshock amplitudes and fault plane changes: a new earthquake precursor? *Science* **201,** 56–59.

Lindh, A. G. and D. M. Boore (1981). Control of rupture by fault geometry during the 1966 Parkfield earthquake, *Bull. Seism. Soc. Am.* **71,** 95–116.

McGarr, A., M. D. Zoback, and T. C. Hanks (1982). Implications of an elastic analysis of in situ stress measurements near the San Andreas fault, *J. Geophys. Res.* **87,** 7797–7806.

Mogi, K. (1963). Some discussions on aftershocks, foreshocks, and earthquake swarms: the fracture of a semi-infinite body caused by an inner stress origin and its relation to earthquake phenomena (third paper), *Bull. Earthquake Res. Inst., Tokyo Univ.* **41,** 615–658.

Real, C. R., T. R. Toppozada, and D. L. Parke (1978). *Earthquake Catalogue of California, January 1, 1900–December 31, 1974,* California Division of Mines and Geology, Sacramento, California.

Richter, C. F. (1958). *Elementary Seismology,* W. H. Freeman and Co., San Francisco, California, 768 pp.

Scheimer, J. F. and R. S. Cocheram (1982). Livermore Valley earthquake sequence January 24–February 29, 1980 (abstract), *Trans. Am. Geophys. Union* **63,** 374.

Scholz, C. H. (1972). Static fatigue of quartz, *J. Geophys. Res.* **77,** 2104–2114.

Sieh, K. E. (1978). Central California foreshocks of the great 1857 earthquake, *Bull. Seism. Soc. Am.* **68,** 1731–1749.

Stein, R. and M. Liwoski (1983). The 1979 Homestead Valley earthquake sequence, California: control

of aftershocks and postseismic deformation, *J. Geophys. Res.* **88,** 6477–6490.

Utsu, T. (1970). Aftershocks and earthquake statistics (II)—Further investigation of aftershocks and other earthquake sequences based on a new classification of earthquake sequences, *J. Faculty Sci., Hikkaido Univ.* **3,** 197–266.

Wyss, M. and J. Brune (1968). Seismic moment, stress and source dimensions for earthquakes in the California-Nevada region, *J. Geophys. Res.* **73,** 4681–4694.

Wyss, M. and T. Hanks (1972). Source parameters of the Borrego Mountain earthquake, *U.S. Geol. Surv. Profess. Paper 787,* 24–30.

Xu, S. X., B. Q. Wang, L. M. Jones, X. F. Ma, and P. W. Shen (1982). The Haicheng earthquake sequence and earthquake swarms—The use of foreshock sequences in earthquake prediction, *Tectonophysics* **85,** 91–105.

Yamashina, K. (1981). Some empirical rules on foreshocks and earthquake prediction, in *Earthquake Prediction: An International Review, Maurice Ewing Series, 4,* D. Simpson and P. Richards, Editors, Am. Geophys. Union, Publ., Washington, D.C., 517–526.

Zoback, M. L. and M. D. Zoback (1980). State of stress in the conterminous United States, *J. Geophys. Res.* **85,** 6113–6156.

LAMONT-DOHERTY GEOLOGICAL OBSERVATORY OF COLUMBIA UNIVERSITY
PALISADES, NEW YORK 10964

Manuscript received 28 November 1983